Article

Engineering of midbrain organoids containing long-lived dopaminergic neurons

TIENG CAULET, Vannary, *et al*.

Abstract

The possibility to generate dopaminergic (DA) neurons from pluripotent stem cells represents an unlimited source of material for tissue engineering and cell therapy for neurodegenerative disease. We set up a protocol based on the generation of size-calibrated neurospheres for a rapid production (3 weeks) of a high amount of DA neurons (>60%) oriented toward a midbrain-like phenotype, characterized by the expression of FOXA2, LMX1A, tyrosine hydroxylase (TH), NURR1, and EN1. By using γ-secretase inhibitors and varying culture time of neurospheres, we controlled maturation and cellular composition of a three-dimensional (3D) engineered nervous tissue (ENT). ENT contained neurons and glial cells expressing various markers of maturity, such as synaptophysin, neuronal nuclei-specific protein (NeuN), and glial fibrillary acidic protein (GFAP), and were electrophysiologically active. We found that 3-week-old neurospheres were optimal to generate 3D tissue containing DA neurons with typical A9 morphology. ENT generated from 4-week-old neurospheres launched glial cell type since astrocytes and myelin could be detected massively [...]

Reference

TIENG CAULET, Vannary, *et al*. Engineering of midbrain organoids containing long-lived dopaminergic neurons. *Stem cells and development*, 2014, vol. 23, no. 13, p. 1535-47

DOI : 10.1089/scd.2013.0442
PMID : 24576173

STEM CELLS AND DEVELOPMENT
Volume 23, Number 13, 2014

DOI: 10.1089/scd.2013.0442

Engineering of Midbrain Organoids Containing Long-Lived Dopaminergic Neurons

Vannary Tieng,[1] Luc Stoppini,[2,3] Sabrina Villy,[4] Marc Fathi,[4] Michel Dubois-Dauphin,[1,*] and Karl-Heinz Krause[1,4,*]

The possibility to generate dopaminergic (DA) neurons from pluripotent stem cells represents an unlimited source of material for tissue engineering and cell therapy for neurodegenerative disease. We set up a protocol based on the generation of size-calibrated neurospheres for a rapid production (3 weeks) of a high amount of DA neurons (>60%) oriented toward a midbrain-like phenotype, characterized by the expression of FOXA2, LMX1A, tyrosine hydroxylase (TH), NURR1, and EN1. By using γ-secretase inhibitors and varying culture time of neurospheres, we controlled maturation and cellular composition of a three-dimensional (3D) engineered nervous tissue (ENT). ENT contained neurons and glial cells expressing various markers of maturity, such as synaptophysin, neuronal nuclei-specific protein (NeuN), and glial fibrillary acidic protein (GFAP), and were electrophysiologically active. We found that 3-week-old neurospheres were optimal to generate 3D tissue containing DA neurons with typical A9 morphology. ENT generated from 4-week-old neurospheres launched glial cell type since astrocytes and myelin could be detected massively at the expense of TH-immunoreactive neurons. All γ-secretase inhibitors were not equivalent; compound E was more efficient than DAPT in generating DA neurons. This DA tissue provides a tool for drug screening, and toxicology. It should also become a useful biomaterial for studies on Parkinson's disease.

Introduction

Human pluripotent stem cells (hPSCs), which include embryonic stem (ES) cells and induced pluripotent stem cells (iPSCs), have the ability of unlimited self-renewal and therefore represent an unlimited source of neurons and glial cells. They hold great promise for tissue engineering applications and for cell replacement therapy in human neurodegenerative diseases [1]. In addition to translational applications, hPSC-based technologies are important for basic research, providing unique insides into mechanisms of human brain development.

Classical two-dimensional (2D) cell culture models are valuable tools for studying cell behavior under stringently controlled conditions. However, the interpretation of cellular response may be skewed by impoverished cell–cell/cell–matrix interactions and cellular morphology. Three-dimensional (3D) tissue model utilizing hPSC-derived neural progenitor cells (NPCs) might overcome these drawbacks in developing stable and long-term culture conditions that optimally mimic the in vivo situation [2–5]. However, 3D tissue engineering still faces major problems like cell survival and cell differentiation, which can be in part solved by the use of presynthesized scaffold [2–4], designed to recreate an extracellular matrix environment [6–9]. However, available scaffolds often do not support neurite outgrowth and do not allow long-term survival of cells [10–12]. The alternative to presynthesized scaffolds is the generation of an extracellular matrix by the cells themselves in 3D tissue culture. Previous studies from our laboratory have shown that this is basically possible [13,14].

NPCs are the obvious starting material to generate engineered nervous tissues (ENTs). Generation of NPCs from PSCs can be obtained either through adherent cell culture protocols or neurosphere suspension-based protocols [15,16]. Neurospheres generated through aggregation of PSCs in suspension have the advantage of generating a miniature autonomous 3D environment containing NPCs and probably also neural stem cells (NSCs). However, variability of cell preparations using this approach is a well-documented drawback. This problem has been solved by using conical cell culture multiwell plates to generate size-homogenous

[1]Department of Pathology and Immunology, University Medical Center, University of Geneva, Geneva, Switzerland.
[2]Hepia, University of Applied Sciences Western Switzerland, Geneva, Switzerland.
[3]Swiss Centre for Applied Toxicology (SCAHT), Geneva, Switzerland.
[4]Department of Genetic and Laboratory Medicine, Geneva Hospitals, Geneva, Switzerland.
*These authors contributed equally to this work.

embryoid bodies (EBs) [17–20]. We then set out to standardize neurosphere producing dopaminergic (DA) neurons. For that purpose, addition of specific small molecules and growth factors, combined with appropriate time culture of NPCs in suspension, was a key factor. In the developing brain, inhibition of Notch pathway results in the cell cycle arrest and differentiation of NPCs [21–23]. In this study, we examined effect of different γ-secretase inhibitors on Notch signaling pathway and particularly we evaluated the impact of two small molecules, compound E and DAPT, on neurosphere differentiation and ENT maturation. Our protocol generates a long-lived nervous tissue containing mature DA neurons from hPSCs with typical A9 morphological characteristics.

Materials and Methods

Culture of undifferentiated hPSCs

Human ES cell line HS415 (passage 17–30, kindly provided by Outi Hovatta, Karolinska Institute, Stockholm, Sweden) and iPSC line NP0026 clone 3 (p10–15, kindly provided by Tomo Saric, University of Cologne, Germany) were cocultured on irradiated (5,000 rad, Irradiator Gamma Cell 3000 Elan, source Cs137) human foreskin feeder cells (CRL-2429; ATCC) in xeno-free/feeder-free media for starting culture. For expansion and differentiation, ES cells were quickly shifted onto human extracellular matrix (Maxgel ECM from Sigma, Cellstart from Invitrogen, or vitronectin from Stemcell Technologies). Different xeno-free media for feeder-free culture and human matrix were tested and gave rise to the same results (mTSR2 medium from Stemcell Technologies, Nutristem from Biological Industries, and Essential 8 from Invitrogen). Media were changed one another day to maintain pluripotency. Cells were passaged with enzymatic procedure (Accutase; Invitrogen) and replated with Rho-associated protein kinase (ROCK) inhibitor (10 μM Y-27632; Ascient Biosciences) during 24 h.

Generation of NPCs and 3D nervous tissue expressing midbrain DA neurons

Neural induction is a first step for NPC generation. Media used to maintain pluripotency features of ES cells were removed and changed to a xeno-free media containing a serum replacement (X-vivo 10; Lonza). To accelerate neural induction step (Fig. 1A), small molecules, LDN193189/SB431542 (LDN/SB = dual-SMAD inhibition cocktail at 0.5 μM/10 μM, respectively; Axon Medchem/Ascent Biosciences) and ROCK inhibitor, essential for sphere formation (10 μM Y-27632; Ascent Biosciences) were added 24 h in 2D culture (day 0). Human ES cells were then detached from matrix and aggregated inside aggrewell plates containing up to 4,700 microwells per well according the model used (Stemcell Technologies). ES cells were recovered enzymatically (Accutase; Invitrogen) as single-cell suspension and evenly distributed among the microwells (day 1) in a medium promoting floor-plate-based midbrain DA neuron induction. Cell aggregates forming spheres were removed by gentle flushing of microwells (day 2). Spheres were cultured in rotation (60 rpm, orbital shaker; Major Science) in six-well plates to prevent spheres sticking together and on the plate. X-vivo 10 medium was gradually shifted to B27 medium [neurobasal medium, B27 1× supplement, 1% non-essential amino acids, 2 mM L-glutamine, 1% penicillin/streptomycin, and 25 μM β-mercaptoethanol (Invitrogen)] starting on day 2. To promote floor-plate-based midbrain DA neuron induction a previously published protocol was modified for suspension culture [24]. Briefly, spheres formed in aggrewell plates were cultured with LDN/SB and regionalization factors, Sonic Hedgehog (SHH, 100 ng/mL; Cell Guidance System), fibroblast growth factor 20 (FGF8, 100 ng/mL; Peprotech), and purmorphamin (2 μM; Calbiochem), from days 1 to 8. CHIR99021 (CHIR, 3 μM; Axon Medchem) was added at day 3 until day 13. Maturation step started at day 10 with dibutyryl cAMP (dbcAMP, 0.5 mM; Sigma), ascorbic acid (0.2 mM; Sigma), growth factors [glial-cell-line-derived neutrophic factor at 10 ng/mL, brain-derived neutrophic factor at 10 ng/mL, transforming growth factor type 3 (TGFβ3) at 1 ng/mL (all from Cell Guidance System), FGF20 at 5 ng/mL (Peprotech), and trichostatin A at 20 nM (Sigma)], and with one of those two following γ-secretase inhibitors: compound E (1 μM; Calbiochem) or DAPT (10 μM; Tocris).

For differentiation in 2D, 3-week spheres were dissociated with Accumax (Millipore) and replated on poly-ornithine- (15 μg/mL; Sigma) and laminin- (2 μg/cm^2; R&D System) coated cover slips (diameter = 0.8 cm) in 24-well plates at 200,000 cells/cm^2 in maturation medium for 1 week before analysis. For production of ENT, neurospheres cultured in suspension during 3 weeks (or 4 weeks) were further seeded on a hydrophilic polytetrafluoroethylene (PTFE) membrane (6-mm diameter and 0.4 μm; Biocell-Interface). This membrane was deposited on a Millicell-CM (0.4 μm) culture plate insert (Millipore). One milliliter of B27 medium supplemented with 20% of knockout serum replacement (Invitrogen) and maturation compounds was added underneath the membrane insert. The cells could be maintained for up to 1 month at air-interface liquid culture before analysis.

Flow cytometry

Undifferentiated ES cells were enzymatically detached as single cells from human matrix and 1- or 3-week-old neurospheres were dissociated (Accutase; Invitrogen). Cells were washed with phosphate-buffered saline before a 10-min fixation step in 4% paraformaldehyde (PFA) at room temperature. To detect intracellular antigens, cells were permeabilized in 1× perm/wash buffer (BD Bioscience) for 10 min, before 30-min incubation in the dark at room temperature with different antibodies (PE Nanog, PerCp-Cy 5.5 Oct ¾ -, and Alexa Fluor 647 Sox2 kit; BD Bioscience). After washing, cells were immediately run or stored at 4°C for 24 h maximum. For each sample run, 10,000 events were recorded and analyzed. Flow cytometry acquisition was performed using FacsCanto I equipment with 488 and 633 lasers (BD Bioscience) and data analysis by Flowjo software.

Gene expression analyses

Total RNA was extracted from ENT using RNeasy midi kit (Qiagen) and reverse transcribed (Takara) for qualitative and quantitative real-time polymerase chain reaction

(qPCR) analysis. Reactions were run on an ABI Prism 7900 HT detection system (Applied Biosystems) for qPCR, based on SYBR green detection. ALAS1, β2 microglobulin, and cyclophilin were used as housekeeping genes and data were normalized to these gene levels. For qualitative PCR, GAPDH and cyclophilin were used as housekeeping genes. For each gene, PCR was performed for 35 cycles with a temperature of 60°C for annealing. Sequences of primers are described in Supplementary Table S1 (Supplementary Data are available online at www.liebertpub.com/scd).

Morphology and immunohistology

After 1 week of culture, 2D cultures on cover slips were fixed in 4% PFA for 10 min at room temperature and washed and processed for conventional immunocytochemistry. ENTs were fixed for 2 h in 4% PFA at 4°C and stored in 2% PFA at 4°C before inclusion in Agar and paraffin embedding. Ten-micrometer-thick transversal ENT sections were processed with cresyl violet for morphological assessment. Both ENT sections and whole ENTs, without paraffin embedding and sectioning, were processed for immunohistochemistry.

Primary antibodies were against Nestin (rabbit polyclonal anti-human, from Chemicon; 1/400), β3-tubulin (mouse monoclonal from Sigma or rabbit polyclonal from Covance; 1/2,000), Synaptophysin (mouse monoclonal from Chemicon; 1/2,000), neuronal nuclei-specific protein (NeuN, mouse monoclonal from Chemicon; 1/1,000), glial fibrillary acidic protein (GFAP, rabbit polyclonal from Dako; 1/2,000), proliferating cell nuclear antigen (PCNA, mouse monoclonal from Dako; 1/100), V-Glut-1 (mouse monoclonal from Chemicon; 1/3,000), GAD-67 (mouse monoclonal from Chemicon; 1/1,000), myelin basic protein (MBP; rabbit polyclonal from Chemicon; 1/1,000), tyrosine hydroxylase (TH; rabbit polyclonal from Millipore; 1/500), FoxA2 (mouse 1/100; Santa Cruz), Lmx1a (rabbit 1/100; Santa Cruz), and Nurr1 (M196, rabbit 1/100; Santa Cruz). Detection of primary antibodies was performed using appropriate species-specific Alexa 488- or Alexa 555-labeled secondary antibodies. Controls included examination of the cell or tissue autofluorescence and omission of the first antibody. Cell nuclei were stained with DAPI. Sections and cell cultures were mounted in Fluorosave (Calbiochem) or Eukitt (Kindler GmbH) and observed with an Axioscop 2 plus microscope equipped with appropriate filters, Axiocam color camera, and Axiovision software (Leitz). Confocal imaging was achieved with an LSM 510 Meta confocal laser scanner and Bitplane SS Imaris 5.7.2 software. Quantitative analysis from immunohistology pictures was made by image J software by measuring color pixels [25].

Electrophysiological recordings

Electrophysiological recordings were obtained at 35°C in culture medium using a porous multi-electrode array (MEA) of 40 electrodes (BioCell-Interface S.A.). Spontaneous activity recordings were typically obtained over 5 min using the same electrodes set as the one used to record evoked activity. Eight recording electrodes and 2 stimulating electrodes (200 μs bipolar stimulation) were selected for any given culture. Paired-pulse evoked field potentials (EFPs) were recorded in response to stimulation of typically 2–4,000 mV every 5 s, with paired-pulse intervals of 50 or 15 ms.

High-pressure liquid chromatography analysis

Dopamine production was analyzed by high-pressure liquid chromatography (HPLC) after extraction from ENTs or 2D cultures in 0.1 N perchloric acid ($HClO_4$). Cells were lysed in a small volume (100 μL) for 15 min at 4°C with a vigorous vortexing every 5 min. Supernatant was recovered after centrifugation and used for dopamine dosage immediately or stored at −20°C. Catecholamines were measured by HPLC with electrochemical detection in coulometric mode. Separation of the analytes was achieved on a reversed-phase column, Symmetry C-18, 5 μm ($4.6 \times 150\,mm^2$) (Waters Corporation), in isocratic mode at a flow rate of 1 mL/min. The coulometric detector parameters, Coulochem III (Thermo scientific), were for conditioning cell at a potential of +200 mV. For analytical cell, an electrode 1 at a potential +100 mV and electrode 2 at a potential of −100 mV were used.

Results

Production of size-calibrated neurospheres and 3D ENTs

Our xeno-free protocol was designed to optimize the production of DA ENTs but could serve as well to generate DA progenitors for transplantation (Fig. 1A). In a first step, PSCs were shifted from culture on human feeder cells onto human extracellular matrix (Fig. 1B, C) to avoid contamination with feeder cells. To initiate neural induction, colonies of undifferentiated PSCs were dissociated into single cells and allowed to re-aggregate in multiwell plates for 24 h. This led to the formation of size-calibrated, homogenous neurospheres (Fig. 1D–F), which were then cultured in suspension under rotating conditions in a six-well plate. We took advantage of recently developed $8 \times 1{,}200$ and of $6 \times 4{,}700$ microwell plates, compatible with large-scale production. It should be mentioned that the number of cells added per microwell was crucial for the success of the experiments; optimal results with respect to reproducibility and uniformity of neurospheres were obtained with 1,000 cells/aggregate. An increase in cell number to 10,000 cells led to increased mortality and to decreased efficiency of small molecules (for example, slow decrease of pluripotency markers, data not shown); when the cell number was decreased below 500 cells per aggregate, neurospheres failed to form (data not shown).

Small-molecule-based protocol helped to improve neural induction without using stromal cells (MS5 or PA6) or expensive component like Noggin. Dual-SMAD inhibition protocol using LDN193189 and SB431542 (LDN/SB) during 8 days gave rise to a rapid loss of pluripotency markers (Nanog and Oct $^{3}/_{4}$) as observed by flow cytometry analysis of neurospheres. In contrast, all cells still expressed Sox2, found in NSC and neural progenitors (Fig. 1G). Addition of SHH/FGF8/purmorphamin/CHIR99021 compounds at the beginning of differentiation phase rapidly oriented neural cells toward floor plate region (Fig. 1A) [24]. ENTs were formed from 3-week-old ~1,000 3-week-old matured neurospheres (corresponding to 1×10^6 cells) deposited on a

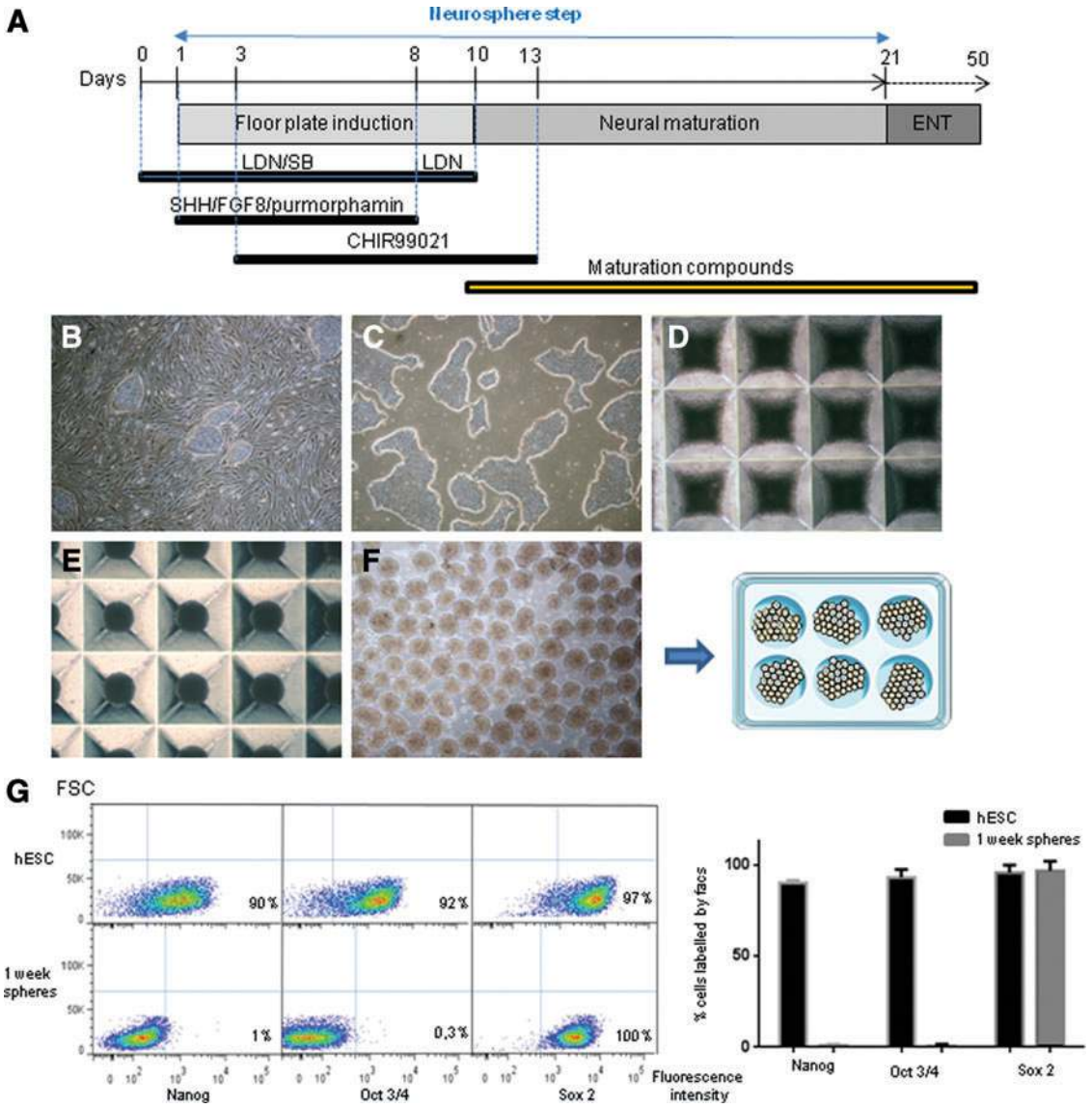

FIG. 1. Principle of the generation of neurospheres. **(A)** Standardized protocol for generation of calibrated neurospheres derived from hPSCs. Diagram of culture conditions **(A)**. hPSCs (HS415 cell line) cultured on human foreskin feeder cells **(B)** were shifted onto human extracellular matrix for expansion **(C)**. Neural induction started at day 0 with cells cultured on human matrix. At day 1, cells detached from matrix as single cells were seeded in microwell plates (Aggrewell™) **(D)**. After 24 h of culture, spherical aggregates, visible within each microwell **(E)**, were harvested for cell culture in suspension in a six-well plate in rotation **(F)**. Pluripotent stem cell markers detected by flow cytometry **(G,** *upper row* and *histograms***)** were expressed in the majority of cells seeded on human matrix (>90% of cells were Oct, Nanog, and Sox2 positive). After 1 week of culture in suspension **(G,** *lower row* and *histograms***)**, sphere analysis showed a rapid loss of pluripotency markers (<1% cells express Oct ¾ or Nanog). A complete conversion of PSCs into NPCs was observed (>98% of cells within neurospheres express Sox2). Flow cytometry data represent mean ± SEM, $n = 5$. LDN: LDN193189, SB: SB431542. Maturation compounds consist of glial-cell-derived neutrophic factor, brain-derived neutrophic factor, transforming growth factor type 3, fibroblast growth factor 20, dibutyryl cAMP, ascorbic acid, trichostatin A, compound E, or DAPT. hPSCs, human pluripotent stem cells; NPC, neural progenitor cell. Color images available online at www.liebertpub.com/scd

semipermeable PTFE membrane under air–liquid interface culture conditions (Fig. 2A). Neurospheres started to fuse within a time frame of hours (Fig. 2B). After 1 month in culture, macroscopically the ENTs appeared as a homogenous tissue with neurite outgrowth at the periphery (Fig. 2C, arrow).

To assess the functionality of the neural tissue, ENTs were placed in perfused chambers onto MEA to record spontaneous electrophysiological activities as well as to EPFs induced by electrical stimulations (Fig. 2D). We observed that the amplitude of the two EFPs was similar when the interval between the stimuli was set at 50 ms (Fig. 2D, 1st top diagram) while there was a clear decrease of the amplitude of the second EFP when the interval is reduced to 15 ms (Fig. 2D, 2nd top diagram). This type of pairing of two pulses in rapid succession led to an inhibition known as

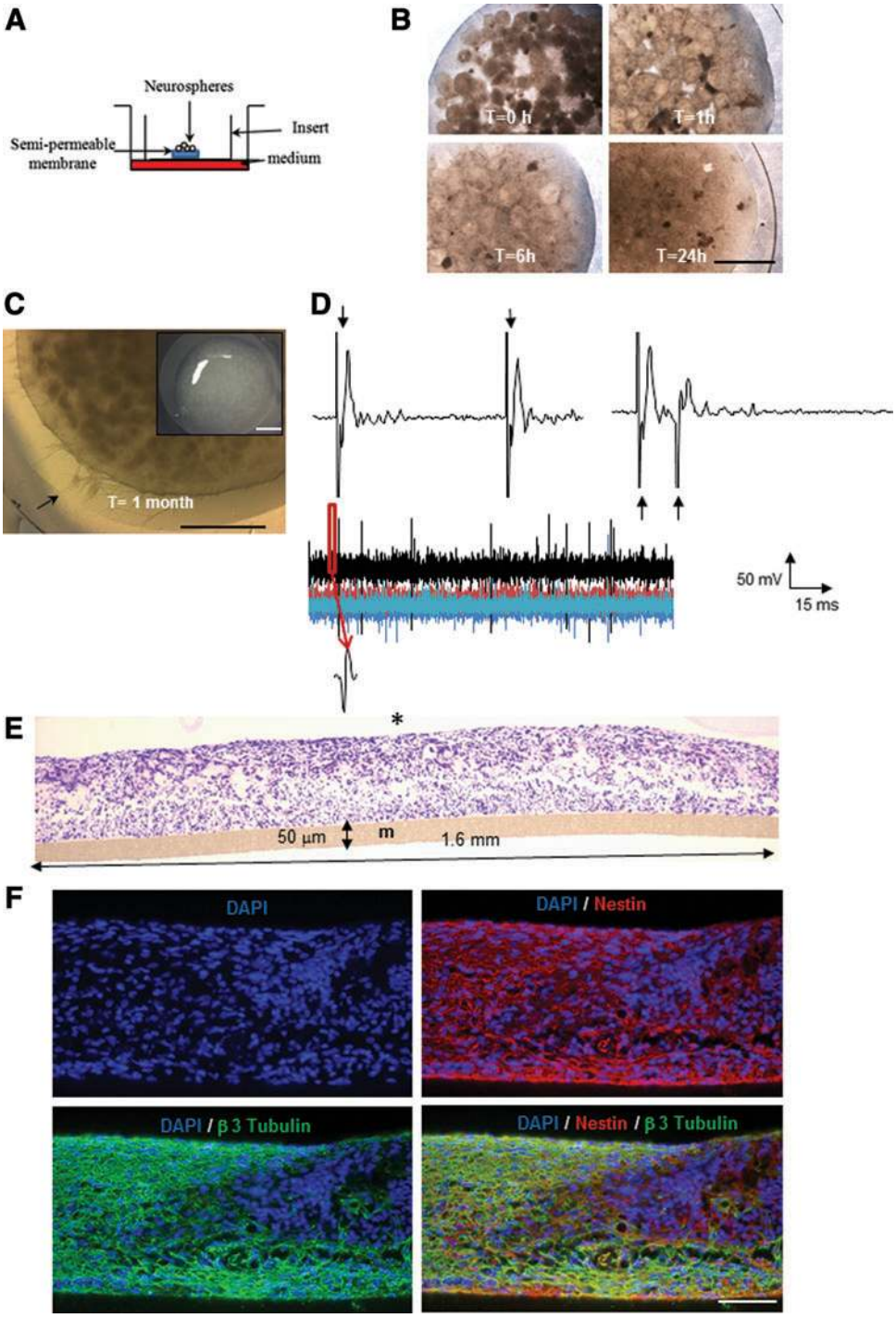

FIG. 2. ENT generation and electrophysiological and morphological analysis. **(A)** Schematic representation of air–liquid interface culture principle. Three- or 4-week-old neurospheres (21 or 28 days) were plated onto PTFE semipermeable membrane. **(B)** Neurospheres fused rapidly and formed a compact cell mass observed in 24 h that gave rise to a 3D engineered neural tissue (ENT). **(C)** Macroscopic (*inset*) and microscopic views of ENT; *arrow* indicates neurite outgrowth in the periphery. **(D)** Electrophysiological analysis of 4-week-old ENT. A paired-pulse stimulation of the ENT with 50-ms interval induced EFP (*1st upper diagram*). Stimulation artifacts are indicated by *arrows*. When interval between the two stimuli was set to 15 ms (*2nd upper diagram*), we observed a net diminution of the second EFP indicating a paired-pulse inhibition. Spontaneous activity from four electrodes **(D,** *lower diagram***)**. An enlargement of one spike is displayed in the *inset*. Dual-smad inhibition with small molecules (LDN/SB) produced a homogenous neural population in 3D culture. ENTs derived from differentiation of hPSCs were fixed in paraformaldehyde after 1 month in culture and sectioned for analysis. **(E)** Cresyl-violet-stained transversal section displayed the homogenous aspect of the 3D culture. Immunohistochemistry showed nestin-immunoreactive cells present in the whole ENT **(F)**, confirming the neural homogeneity of the 3D structure. β3-Tubulin immunoreactivity was distributed heterogeneously; it was absent from rosette-like structures that were nestin immunoreactive. The *asterisk* (*) indicates the air–liquid culture interface and (m) indicates the PTFE membrane. Scale bar: **(F)** 50 µm, **(B, C)** 1 mm. 3D, three-dimensional; EFP, evoked field potential; ENT, engineered nervous tissue; PTFE, polytetrafluoroethylene. Color images available online at www.liebertpub.com/scd

paired-pulse inhibition and was generally due to the recurrent inhibition of the subsequent response initiated in the neural network by the second stimulus delivered shortly (15 ms) after the first one. Many individual or bursting extracellular action potentials could be recorded.

Cresyl-violet-stained transversal section of ENTs (Fig. 2E) displayed a homogenous aspect, with cells surrounded by a matrix and without endoderm- or mesoderm-derived structures observed. Cells were nestin and β3 tubulin immunoreactive, confirming the strict neural identity of the ENTs (Fig. 2F).

DA neuron maturation in 2D culture and in ENTs

The orientation of neurospheres toward a midbrain-like phenotype was carried out rapidly by the addition of regionalization factors, such as SHH, FGF8, purmorphamin, and CHIR99021, GSK3β, a glycogen synthetase inhibitor, at the beginning of neural induction (Fig. 1A). Expression of floor plate markers (*FOXA2* and *LMX1A*) and midbrain markers (*NURR1* and *EN1*) was detected from 3-week-old neurospheres (Fig. 3A). Variation in TH expression was assessed in DA-oriented ENTs generated from 2-, 3-, and 4-week-old neurospheres. After 1 week of 3D culture, optimal expression of TH was detected in ENTs issued from 3-week-old neurospheres (Fig. 3B). We also compared two ways to generate NPCs for ENTs; neurosphere-derived NPCs generated more TH than NPCs from 2D culture (Fig. 3C). Cells in 3-week neurospheres were examined after complete dissociation of 3-week neurospheres and plating onto 2D polyornithin/laminin surface; after 1 week of culture, ~80% of cells express the floor plate markers FoxA2 and Lmx1a. More than 60% of cells were TH-immunoreactive cells mostly coexpressing Nurr1 and FoxA2 nuclear markers (Fig. 3D). TH cells were rarely detected or the number decreased when neurospheres were dissociated and plated from 2- or 4-week-old neurospheres, respectively (data not shown). Three-week-old neurospheres were used to generate ENTs. Surprisingly we observed a clear reduction of cells expressing the previous markers (FoxA2, Lmx1a, TH, and Nurr1) and the number of TH cells fell down from >60% to ~30% after 1 week of culture, an observation confirmed over this period and up to 1-month culture (data not shown) (Fig. 3E). Other surprising observations were the loss of colocalization of TH and FoxA2 markers for a lot of cells and the re-localization of Nurr1 from nucleus to cytoplasm (Fig. 3E).

We then assessed the impact of 3D environment on the morphology of TH-immunoreactive neurons; 3-week-old neurospheres were either dissociated and plated onto laminin surface for further culture in 2D or deposited on PTFE membrane to form ENTs (see Materials and Methods section). Immunohistochemistry showed TH-immunoreactive neurons with varicose neurites (Fig. 4A, arrow), typical of A9 neurons, which were not observed in 2D culture [26–28]. Typically, ENTs gave rise to large peripheral bundles of neurite immunoreactive for β3 tubulin and TH (Fig. 4B, dotted outline). This characteristic was not observed in 2D culture with the same ES line (Fig. 3D and data not shown). This observation was depended on cell line used as one iPSC line did not produce these peripheral bundles (Fig. 4B, lower panel).

The presence of DA neurons in ENT culture was also assessed by their ability to synthesize dopamine. For that purpose, ENTs and terminal 2D culture were lysed in perchloric acid and supernatants were submitted to HPLC analysis. ENTs and 2D culture produced the same concentration of dopamine for the same quantity of cells analyzed (Fig. 4C), although TH cell ratio is lower in ENT conditions.

Impact of Notch inhibition pathway on ENT maturity

The impact of the Notch inhibition pathway on neural maturation of neurospheres was assessed by comparing the effect of dimethyl sulfoxide (DMSO) and γ-secretase inhibitor compound E (Fig. 5A). Compound E was added to the neurospheres between days 10 and 21 in suspension culture, and subsequently during ENT formation. In 1-month-old ENTs, synaptophysin immunoreactivity was not detected under control DMSO condition but, in contrast, it was abundant when compound E was added during the neural maturation phase. Similarly, β3-tubulin immunoreactivity and NeuN immunoreactivity, a marker of maturity for neurons, were massively expressed under compound E influence. There was no obvious influence of compound E on the distribution of PCNA-immunoreactive cells. However, it is worth noting that under DMSO conditions only few areas were GFAP positive and hence many PCNA-positive cells were GFAP negative, possibly corresponding to nestin-immunoreactive neural progenitors. In contrast, under compound E, GFAP-immunoreactive cells were abundant and many of the PCNA-immunoreactive cells were also GFAP positive. Thus, under compound E conditions, proliferating cells may predominantly be astrocytes.

Another striking effect of compound E was the enhancement of TH- immunoreactive cells (Fig. 5A), However, other γ-secretase inhibitors, such as DAPT, were not as efficient in generating TH-immunoreactive neurons. Thus, a higher number of TH-immunoreactive neurons with long neurites were produced under compound E influence whereas rare TH-immunoreactive cells were detected under DAPT treatment (Fig. 5B).

Immunoreactivities for the vesicular glutamate transporter VGLUT1 for glutamatergic neurons were strongly enhanced under compound E, suggesting the development of specific subtypes of mature neurons. No effect of compound E on GAD67 expression, marker for gabaergic neurons, was detected (Fig. 5A).

The maturity of ENTs was also influenced by the age of neurospheres used to prepare them. MBP, a marker for myelin, was poorly detected in ENTs from 3-week-old neurospheres raised in both DMSO and compound E conditions (data not shown). In contrast, compound E-treated 4-week-old neurospheres produced ENT expressing abundantly MBP immunoreactivity, a feature absent when neurospheres were DMSO treated (Fig. 5A).

Discussion

In this study we developed a technology that allows engineering of mature and patterned neural tissues from hPSCs. The nervous tissue generated in this study contained DA and glutamatergic neurons. It showed spontaneous and evoked electrical activity and should be of interest for

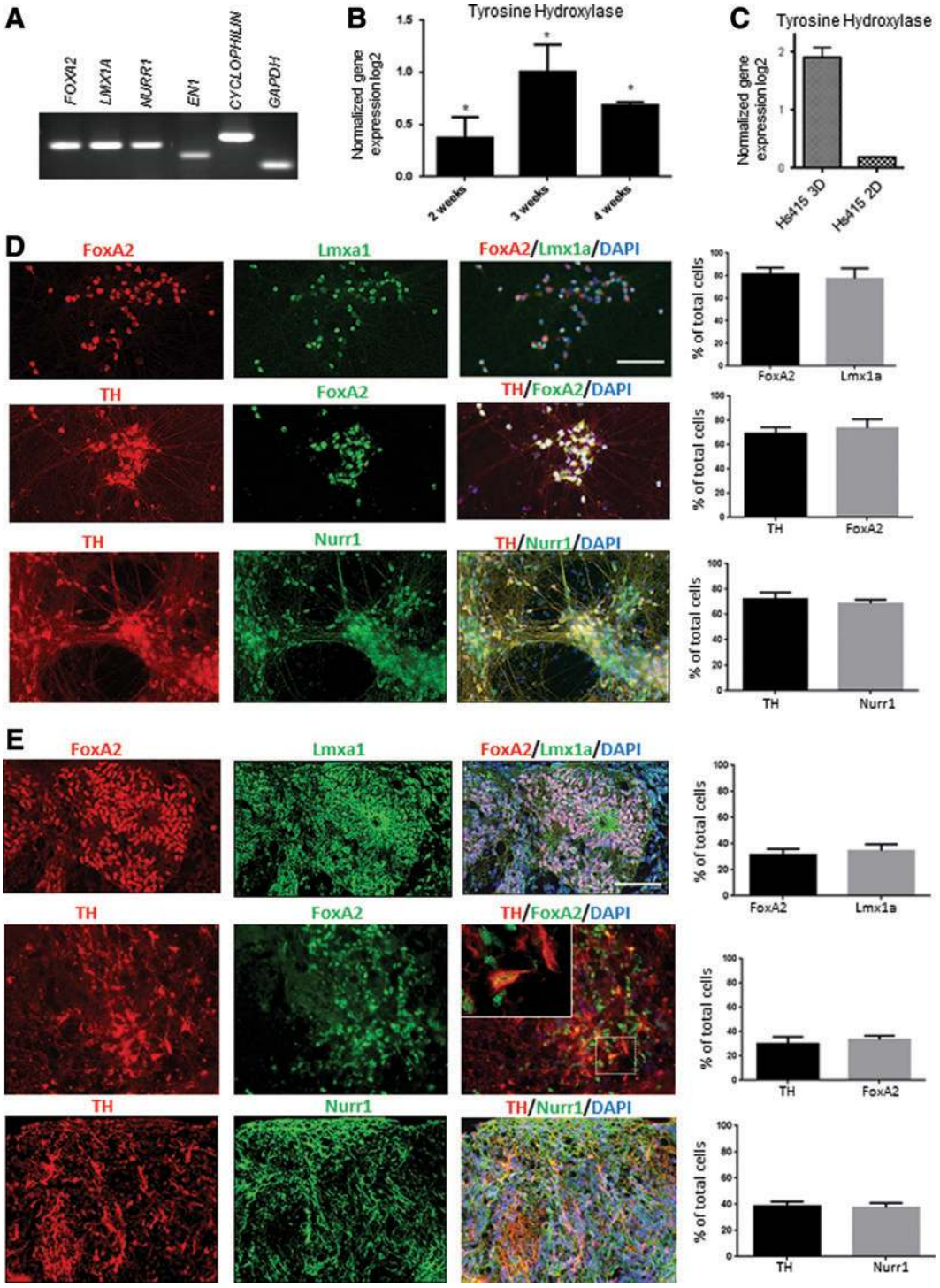

FIG. 3. Patterning toward midbrain development. **(A)** Expression of floor plate markers (*FOXA2* and *LMX1A*) and midbrain markers (*NURR1* and *EN1*) was detected in 3-week-old neurospheres by qualitative PCR. *GAPDH* and *CYCLOPHILIN* served as housekeeping genes. **(B)** *TH* expression in DA ENTs issued from 2-, 3-, and 4-week-old neurospheres was evaluated by quantitative real-time PCR. After 1 week of culture, optimal expression of *TH* was detected in ENTs issued from 3-week-old neurospheres (data represent mean ± SEM, $n = 3$, significance level $^*P < 0.05$, one-way ANOVA). **(C)** Comparison of the dopaminergic potential of two ways to produce NPCs for ENT production. NPCs from neurospheres (HS415 3D) generated more *TH* expression in ENTs than NPCs from HS415 2D culture (data represent mean ± SEM, $n = 3$, significance level $P < 0.001$, Student's *t*-test). **(D)** Complete dissociation of 3-week-old neurospheres and plating onto 2D polyornithin/laminin surface gave rise to high amount of cells expressing immunoreactivity for floor plate markers FoxA2 and Lmx1a (>80%) and a high amount of TH-immunoreactive cells coexpressing FoxA2 and Nurr1 (>70%). **(E)** When 3-week-old neurospheres are used to form ENTs, the cells show a decrease of expression for all these markers with a change in localization of Nurr1, becoming cytoplasmic, and FoxA2 and TH less colocalized (for 2D plating and ENT, immunofluorescence and cell counting, mean ± SEM, $n = 3$). PCR, polymerase chain reaction; TH, tyrosine hydroxylase. Color images available online at www.liebertpub.com/scd

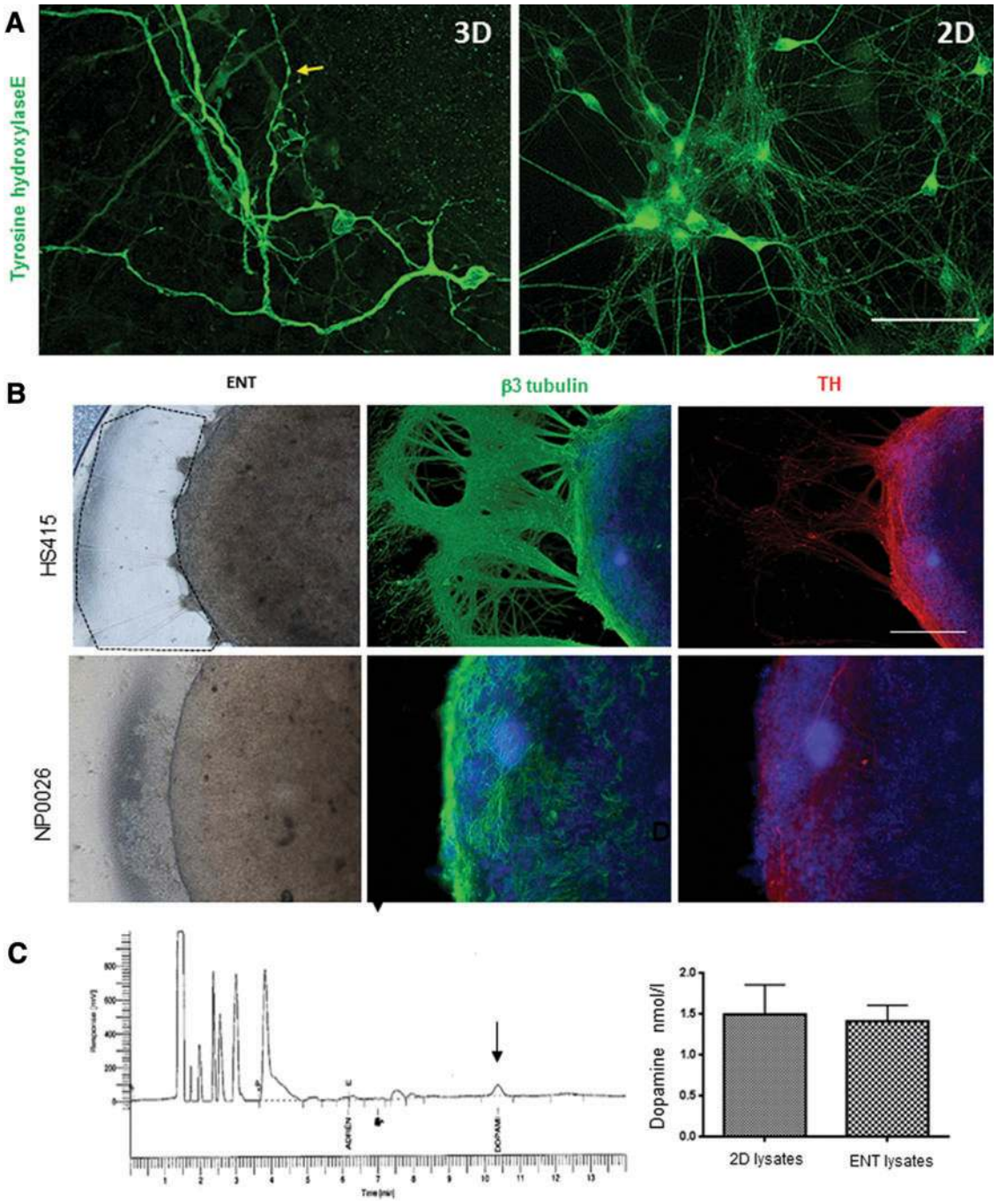

FIG. 4. Characterization of TH cells present in 2D and ENT cultures. **(A)** TH-immunoreactive neuron morphology inside an ENT derived from neurosphere culture analyzed by confocal microscopy; the *arrow* shows typical varicosities of DA neurons (*left-hand-side picture*). TH-immunoreactive neuron morphology on 2D culture surface coated with laminin after dissociation of neurospheres (*right-hand-side picture*). **(B)** Top view of total ENT immunostained for β3-tubulin or TH and generated from hES cells (*upper row*) or from iPSCs (*lower row*). In the case of hES cells large peripheral bundles of neurites were found outgrowing from ENT (delimited by *dotted outline*). These neurite extensions were immunoreactive for β3-tubulin and TH. In the case of iPSC line no neurite extensions were observed although β3-tubulin and TH were detected inside the ENT. **(C)** Analysis of dopamine present in 2D cultures and ENT: representative high-pressure liquid chromatography chromatogram from ENT lysate for adrenaline and dopamine analysis (*arrow, left side of the figure*) and quantification of dopamine present in ENT ($n=5$) and 2D ($n=3$) culture lysates (*right-hand-side picture*). Each ENT was formed from 10^6 cells (DA quantification was reported for 0.5×10^6 cells compare with 2D culture containing 0.5×10^6 cells/well). The cell nuclei are stained in *blue* by DAPI. Scale bar: **(A)** 50 μm, **(B)** 1 mm. DA, dopaminergic; hES, human embryonic stem. Color images available online at www.liebertpub.com/scd

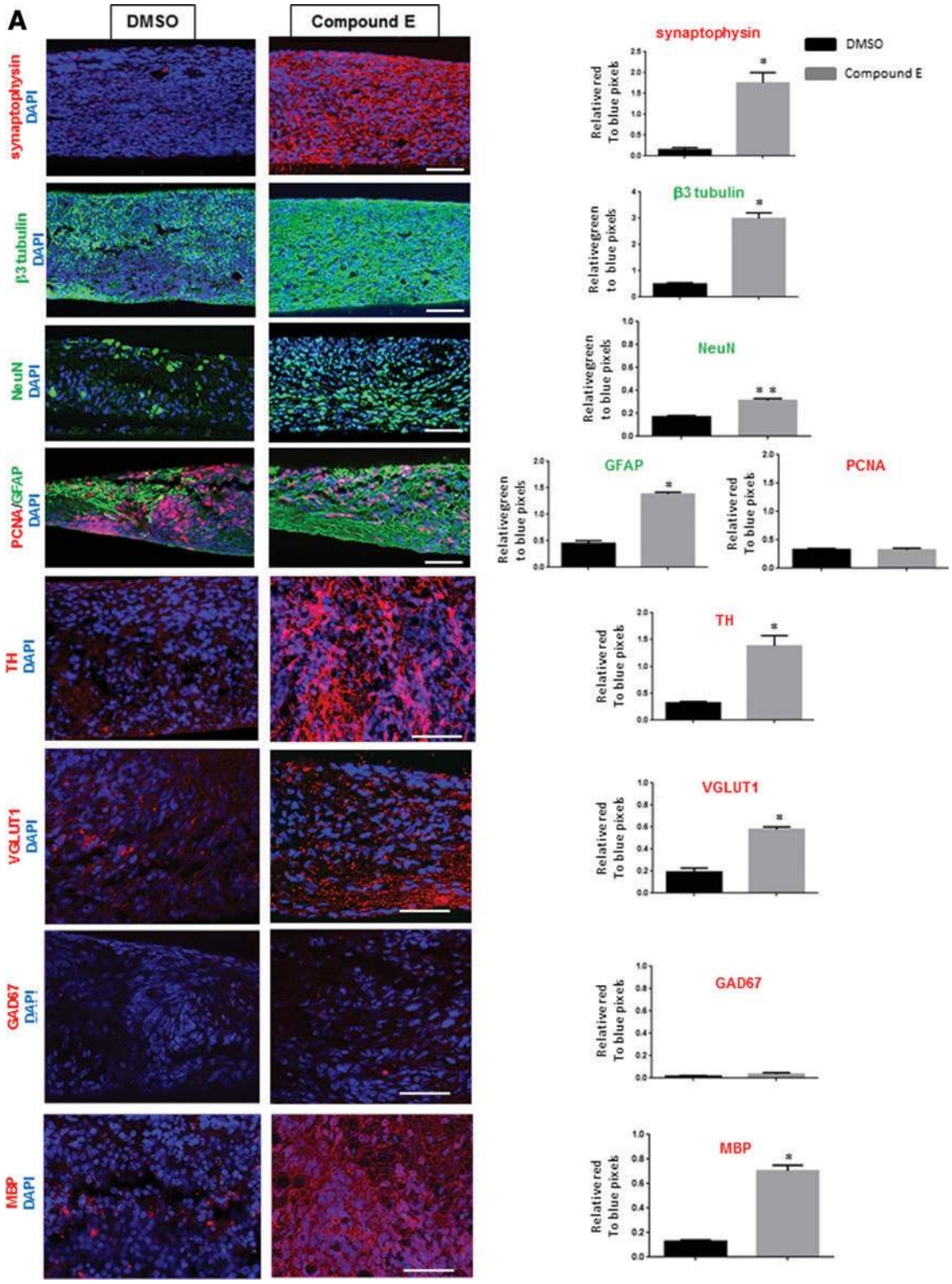

FIG. 5. γ-Secretase inhibitor effects on ENT maturation. **(A)** Compound E effect on 1-month-old ENT generated from 3-week-old neurospheres was compared with DMSO control (immunohistochemical analysis). Compound E produced a more mature ENT phenotype characterized here by a higher expression of synaptophysin, β3 tubulin, NeuN, TH, GFAP, and VGLUT1 immunoreactivities. No clear Gad67-immunoreactive cells were observed. PCNA immunoreactivities were similar in both conditions. ENT generated from 4-week-old neurospheres gave rise to MBP immunoreactivity that was strongly enhanced by compound E. Comparison of compound E effect versus DMSO is made by relative *green* or *red pixels* to *blue pixels* = DAPI, mean ± SEM, $n = 3$, Student's *t*-test, $^{*}P < 0.001$, $^{**}P < 0.05$. **(B)** Compound E-treated ENT issued from 3-week-old neurospheres shows a dense network of TH-immunoreactive neurons in comparison to DAPT-treated ENT (comparison made by relative *green pixels* = TH to *blue pixels* = DAPI, $n = 3$, $^{*}P < 0.001$). The cell nuclei are stained in *blue* with DAPI. Scale bar **(A, B)** 50 μm. DMSO, dimethyl sulfoxide; GFAP, glial fibrillary acidic protein; MBP, myelin basic protein; NeuN, neuronal nuclei-specific protein; PCNA, proliferating cell nuclear antigen. Color images available online at www.liebertpub.com/scd

(Figure continued →)

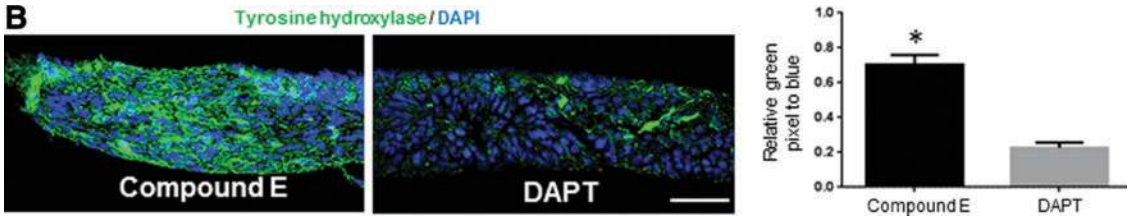

FIG. 5. (Continued).

pathophysiological, pharmacological, and toxicological studies. Unlike ENT mouse model [13], human model did not show spatially organized structure but was quite homogenous in cellular composition. However, without the use of ''dual-SMAD inhibition protocol'' and γ-secretase inhibitors, ENT model resulted in immature neural-tube-like structures, immature neurons, and heterogeneous neural tissue contaminated by mesenchymal structures [14]. Key elements for the generation of such tissues include highly standardized neurosphere generation, use of small molecules to control neural induction and neural maturation, as well as timed addition of regionalization factors. The controlled induction and maturation of neural precursors in a neurosphere suspension culture is one of the key findings of our study. To achieve this goal, several technologies needed to be combined: (1) generation of neurospheres using single-cell suspension of pluripotent stem cells, (2) size calibration of developing neurospheres, and (3) sequential use of small-molecule modulators to optimize neural induction and maturation.

Classically, generation of neurospheres consists of unwieldy methods with manual scraping of adherent ES cells and/or mechanically cut of rosette structures containing NPCs, in order to release clumps of cell aggregates in suspension culture [29,30]. These approaches were used to compensate for the poor survival of hPSCs as single cells. However, the differentiation achieved through these approaches was not sufficiently controlled and led to neurospheres that were heterogeneous in size and shape. We therefore used a single-cell approach, achieved through enzymatic dissociation of hPSC colonies. The crucial addition of ROCK inhibitor allows survival of hPSC single cells [31] and facilitates their spontaneous aggregation. When growing cells as spheres in suspension, sphere size influences differentiation potential [17]. This has been particularly well documented for EBs, where large spheres tended to form meso/endoderm layers while small spheres tended to form ectoderm. To avoid this problem EBs were size calibrated [20]. Combining microwell plates with the use of small molecules like ROCK, BMP, and TGFβ inhibitors (referred as dual-SMAD inhibition protocol) [15,32] we were able to generate size-calibrated neurospheres containing exclusively NPCs. Hence, ENT generation from NPCs was also reproducible, an important feature for the development of reproducible and quantitative pharmacological and toxicological investigations with this in vitro model.

In our work we have oriented neurosphere differentiation to generate midbrain-like DA neurons. Three-dimensional neurosphere structure was more powerful over 2D culture to generate rapidly a higher amount of DA neurons (>60% at day 28 of differentiation) in comparison to the 2D original protocol developed by Kriks' and colleagues (~20% of cells were TH in day 25 and ~75% at day 50) [24]. Three-dimensional cultures of DA neuroprecursors harvested from fetal brain result in higher levels of survival, longer neurite outgrowth, and different patterns of differentiation when compared with 2D monolayers [33–36].

ENT differentiation toward midbrain was characterized by TH, FoxA2, and Lmx1a staining, localized preferentially inside rosette-like immature structures whereas Nurr1 was preferentially detected outside the immature structures (Fig. 3E). These observations concur with in vivo observations; at the beginning of midbrain development FoxA2 and Lmx1a are expressed in the floor plate but are downregulated in adult brain. Nurr1 appears later during midbrain formation and remains in adult brain [37,38]. As such our ENT model mimics here part of midbrain development. Unexpected data came from localization of Nurr1 immunoreactivity inside ENTs; while it was localized in the nucleus of TH-immunoreactive cells in 2D culture (plating of cells coming from dissociated neurospheres), in ENT, Nurr1 immunoreactivity was mainly localized in the cytoplasm. Oxidative stress [39] or toxicity [40] could explain this redistribution. However, in the brain and depending on the region considered, Nurr1 could be also localized in the cell cytoplasm [41]. The lower number of TH cells observed in ENT culture and the lack of coexpression with FoxA2 could be explained as well by stress conditions related to the 3D culture. One explanation concerning the higher number of TH cells in 2D culture after neurosphere dissociation in comparison to ENT culture could be due to laminin-coated plates in 2D culture; the matrix could participate in increasing the survival of TH cells. On the other hand, it seemed that 3D conditions favored maturation of TH-immunoreactive neurons; we observed TH neurons with varicose neurites inside ENTs (varicose neurites being one morphologic sign of mature neurons in vivo), absent in 2D culture [26–28]. Another favorable observation is a higher level of DA inside ENT structure relative to the lower number of TH cells in comparison to the 2D culture.

The use of a γ-secretase inhibitor (compound E) seemed to be another key element to accelerate ENT maturation and DA neuron production by acting likely through inhibition of the Notch pathway [21–23]. Interestingly by using another γ-secretase inhibitor, DAPT, DA neurons were rarely detected in ENT structure. An explanation could be provided by the fact that γ-secretase signaling involves ~50 substrates known to be processed through this enzyme [42,43]. For both compounds we have used nontoxic concentrations

referenced as optimal for neuronal differentiation and for Notch pathway inhibition [24]. However, DAPT could influence specifically DA neuron population in 3D but not in 2D (this work and Ogura et al. [44]). So, all γ-secretase inhibitors are not equivalent in terms of DA neuronal differentiation.

We found that the age of NPCs in suspension culture could influence cell maturation and cellular composition of ENTs toward gliogenic cells. During nervous system development, neural precursors first generate neurons and then switch to glia cells [45]. We observed that prolonged culture time in suspension from 3 to 4 weeks seemed to be important for shifting toward gliogenic step and a loss of TH expression (Supplementary Fig. S1). Indeed, MBP immunoreactivity reflecting the presence of oligodendrocytes was only detected in ENTs issued from 4-week-old neurospheres. Significant advances have been made since the first neural differentiation protocols from hPSCs. Among many of them, coculture with stromal cell lines (MS5 and PA6) was considered as a gold standard for neural differentiation of mouse and human ES lines before the introduction of small molecules [46,47]. Since hPSC-derived nervous tissue may also serve in the context of regenerative medicine and cell replacement therapy, we have designed a fully clinical-grade protocol using for each step of differentiation well-defined and xeno-free components. Our human ENT model could also serve for prescreening cell lines before transplantation. We made two main observations using ENT: (1) differences between γ-secretase inhibitors, compound E and DAPT, in terms of TH expression and (2) difference between neurite outgrowth depending on the cell lines used (one iPSC line tested lacked neurite outgrowth). These two parameters could be important for transplantation as low number of TH cells and lack of striatum innervation could lead to a failure of Parkinson phenotype reversion. For in vitro or in vivo utilizations, the necessity to yield a neural population devoid of undifferentiated or ill-differentiated cells is a priority. By using ENTs, it is possible to evaluate the degree of differentiation and the phenotypical identity of cell preparation without using animals. ENT model could mimick events occurring in vivo such as the dramatic decline of TH cells following transplantation. Reports mentioned only 3% to 6% of TH cells after transplantation although a high yield obtained in in vitro 2D culture [24,48].

Conclusions

We have designed a protocol to generate 3D DA-engineered human nervous tissue from hPSC-derived NPCs capable of long-term survival. This 3D nervous tissue is suitable to determine conditions producing an optimal differentiation of hPSCs, devoid of potentially dangerous undifferentiated or ill-differentiated cells before transplantations; it allows investigation of the choice of cell lines, the choice of small molecules for neurochemical orientation of neurons and their maturation. All these aspects are important in preclinical studies before considering further cell replacement therapies. In addition, this easy-to-handle 3D structure is also suitable for a broad array of neurodegenerative diseases and more generally is an attractive model for Parkinson and myelin-related diseases. In vitro pharmacological, toxicological, and developmental investigations are part of potential applications.

Acknowledgments

The authors thank Fonds National de la Recherche Suisse (FNRS; Prometheus consortium, Sinergia project), Clayton Foundation, Carigest SA, for financial support. The authors also thank Olivier Brun and François Prodon (Faculty of Medicine, Geneva) for their help in confocal microscopy and image J analysis, respectively; Outi Hovatta from Karolinska Institute, Stockholm, Sweden, for providing human ES cell line HS415; and Tomo Saric from University of Cologne, Germany, for providing iPSC line NP0026.

Author Disclosure Statement

The authors have no competing financial interests.

References

1. Orlacchio A, G Bernardi, A Orlacchio and S Martino. (2010). Stem cells: an overview of the current status of therapies for central and peripheral nervous system diseases. Curr Med Chem 17:595–608.
2. Dutta RC and AK Dutta. (2009). Cell-interactive 3D-scaffold; advances and applications. Biotechnol Adv 27:334–339.
3. Subramanian A, UM Krishnan and S Sethuraman. (2009). Development of biomaterial scaffold for nerve tissue engineering: Biomaterial mediated neural regeneration. J Biomed Sci 16:108.
4. Tibbitt MW and KS Anseth. (2009). Hydrogels as extracellular matrix mimics for 3D cell culture. Biotechnol Bioeng 103:655–663.
5. Brito C, D Simao, I Costa, R Malpique, CI Pereira, et al. (2012). 3D cultures of human neural progenitor cells: dopaminergic differentiation and genetic modification. [corrected]. Methods 56:452–460.
6. Dewitt DD, SN Kaszuba, DM Thompson and JP Stegemann. (2009). Collagen I-matrigel scaffolds for enhanced Schwann cell survival and control of three-dimensional cell morphology. Tissue Eng Part A 15:2785–2793.
7. Drury JL and DJ Mooney. (2003). Hydrogels for tissue engineering: scaffold design variables and applications. Biomaterials 24:4337–4351.
8. Madison R, CF da Silva, P Dikkes, TH Chiu and RL Sidman. (1985). Increased rate of peripheral nerve regeneration using bioresorbable nerve guides and a laminin-containing gel. Exp Neurol 88:767–772.
9. Wells MR, K Kraus, DK Batter, DG Blunt, J Weremowitz, et al. (1997). Gel matrix vehicles for growth factor application in nerve gap injuries repaired with tubes: a comparison of biomatrix, collagen, and methylcellulose. Exp Neurol 146:395–402.
10. Borkenhagen M, JF Clemence, H Sigrist and P Aebischer. (1998). Three-dimensional extracellular matrix engineering in the nervous system. J Biomed Mater Res 40:392–400.
11. Dillon GP, X Yu, A Sridharan, JP Ranieri and RV Bellamkonda. (1998). The influence of physical structure and charge on neurite extension in a 3D hydrogel scaffold. J Biomater Sci Polym Ed 9:1049–1069.
12. Mahoney MJ and KS Anseth. (2006). Three-dimensional growth and function of neural tissue in degradable polyethylene glycol hydrogels. Biomaterials 27:2265–2274.
13. Dubois-Dauphin ML, N Toni, SD Julien, I Charvet, LE Sundstrom, et al. (2010). The long-term survival of *in vitro* engineered nervous tissue derived from the specific neural

differentiation of mouse embryonic stem cells. Biomaterials 31:7032–7042.
14. Preynat-Seauve O, DM Suter, D Tirefort, L Turchi, T Virolle, et al. (2009). Development of human nervous tissue upon differentiation of embryonic stem cells in three-dimensional culture. Stem Cells 27:509–520.
15. Chambers SM, CA Fasano, EP Papapetrou, M Tomishima, M Sadelain, et al. (2009). Highly efficient neural conversion of human ES and iPS cells by dual inhibition of SMAD signaling. Nat Biotechnol 27:275–280.
16. Kirkeby A, J Nelander and M Parmar. (2012). Generating regionalized neuronal cells from pluripotency, a step-by-step protocol. Front Cell Neurosci 6:64.
17. Bauwens CL, R Peerani, S Niebruegge, KA Woodhouse, E Kumacheva, et al. (2008). Control of human embryonic stem cell colony and aggregate size heterogeneity influences differentiation trajectories. Stem Cells 26:2300–2310.
18. Bratt-Leal AM, RL Carpenedo and TC Mc Devitt. (2009). Engineering the embryoid body microenvironment to direct embryonic stem cell differentiation. Biotechnol Prog 25: 43–51.
19. Hwang YS, BG Chung, D Ortmann, N Hattori, HC Moeller, et al. (2009). Microwell-mediated control of embryoid body size regulates embryonic stem cell fate via differential expression of WNT5a and WNT11. Proc Natl Acad Sci U S A 106:16978–16983.
20. Ungrin MD, C Joshi, A Nica, C Bauwens and PW Zandstra. (2008). Reproducible, ultra high-throughput formation of multicellular organization from single cell suspension-derived human embryonic stem cell aggregates. PLoS One 3:e1565.
21. Oya S, G Yoshikawa, K Takai, JI Tanaka, S Higashiyama, et al. (2009). Attenuation of Notch signaling promotes the differentiation of neural progenitors into neurons in the hippocampal CA1 region after ischemic injury. Neuroscience 158:683–692.
22. Borghese L, D Dolezalova, T Opitz, S Haupt, A Leinhaas, et al. (2010). Inhibition of notch signaling in human embryonic stem cell-derived neural stem cells delays G1/S phase transition and accelerates neuronal differentiation *in vitro* and *in vivo*. Stem Cells 28:955–964.
23. Oishi K, S Kamakura, Y Isazawa, T Yoshimatsu, K Kuida, et al. (2004). Notch promotes survival of neural precursor cells via mechanisms distinct from those regulating neurogenesis. Dev Biol 276:172–184.
24. Kriks S, JW Shim, J Piao, YM Ganat, DR Wakeman, et al. (2011). Dopamine neurons derived from human ES cells efficiently engraft in animal models of Parkinson's disease. Nature 480:547–551.
25. Brennand KJ, A Simone, J Jou, C Gelboin-Burkhart, N Tran, et al. (2011). Modelling schizophrenia using human induced pluripotent stem cells. Nature 473:221–225.
26. Finkelstein DI, D Stanic, CL Parish, D Tomas, K Dickson, et al. (2000). Axonal sprouting following lesions of the rat substantia nigra. Neuroscience 97:99–112.
27. Kung L, M Force, DJ Chute and RC Roberts. (1998). Immunocytochemical localization of tyrosine hydroxylase in the human striatum: a postmortem ultrastructural study. J Comp Neurol 390:52–62.
28. Bedard C, MJ Wallman, E Pourcher, PV Gould, A Parent, et al. (2011). Serotonin and dopamine striatal innervation in Parkinson's disease and Huntington's chorea. Parkinsonism Relat Disord 17:593–598.
29. Dottori M and MF Pera. (2008). Neural differentiation of human embryonic stem cells. Methods Mol Biol 438: 19–30.
30. Zhang XQ and SC Zhang. (2010). Differentiation of neural precursors and dopaminergic neurons from human embryonic stem cells. Methods Mol Biol 584:355–366.
31. Watanabe K, M Ueno, D Kamiya, A Nishiyama, M Matsumura, et al. (2007). A ROCK inhibitor permits survival of dissociated human embryonic stem cells. Nat Biotechnol 25:681–686.
32. Zhou J, P Su, D Li, S Tsang, E Duan, et al. (2010). High-efficiency induction of neural conversion in human ESCs and human induced pluripotent stem cells with a single chemical inhibitor of transforming growth factor beta superfamily receptors. Stem Cells 28:1741–1750.
33. Fawcett JW, RA Barker and SB Dunnett. (1995). Dopaminergic neuronal survival and the effects of bFGF in explant, three dimensional and monolayer cultures of embryonic rat ventral mesencephalon. Exp Brain Res 106:275–282.
34. Choi HK, L Won and A Heller. (1993). Dopaminergic neurons grown in three-dimensional reaggregate culture for periods of up to one year. J Neurosci Methods 46:233–244.
35. Pardo B and P Honegger. (2000). Differentiation of rat striatal embryonic stem cells *in vitro*: monolayer culture vs. three-dimensional coculture with differentiated brain cells. J Neurosci Res 59:504–512.
36. O'Connor SM, DA Stenger, KM Shaffer, D Maric, JL Barker, et al. (2000). Primary neural precursor cell expansion, differentiation and cytosolic Ca(2+) response in three-dimensional collagen gel. J Neurosci Methods 102: 187–195.
37. Ferri AL, W Lin, YE Mavromatakis, JC Wang, H Sasaki, et al. (2007). Foxa1 and Foxa2 regulate multiple phases of midbrain dopaminergic neuron development in a dosage-dependent manner. Development 134:2761–2769.
38. Nakatani T, M Kumai, E Mizuhara, Y Minaki and Y Ono. (2010). Lmx1a and Lmx1b cooperate with Foxa2 to coordinate the specification of dopaminergic neurons and control of floor plate cell differentiation in the developing mesencephalon. Dev Biol 339:101–113.
39. Garcia-Yague AJ, P Rada, AI Rojo, I Lastres-Becker and A Cuadrado. (2013). Nuclear import and export signals control the subcellular localization of Nurr1 protein in response to oxidative stress. J Biol Chem 288:5506–5517.
40. Boldingh Debernard KA, GH Mathisen and RE Paulsen. (2012). Differences in NGFI-B, Nurr1, and NOR-1 expression and nucleocytoplasmic translocation in glutamate-treated neurons. Neurochem Int 61:79–88.
41. Ojeda V, JA Fuentealba, D Galleguillos and ME Andres. (2003). Rapid increase of Nurr1 expression in the substantia nigra after 6-hydroxydopamine lesion in the striatum of the rat. J Neurosci Res 73:686–697.
42. Haapasalo A and DM Kovacs. (2011). The many substrates of presenilin/gamma-secretase. J Alzheimers Dis 25:3–28.
43. Yang MS, JS Hong, ST Kim, KY Lee, KW Park, et al. (2011). Among gamma-secretase substrates Notch1 alone is sufficient to block neurogenesis but does not confer self-renewal properties to neural stem cells. Biochem Biophys Res Commun 404:133–138.
44. Ogura A, A Morizane, Y Nakajima, S Miyamoto and J Takahashi. (2013). Gamma-secretase inhibitors prevent overgrowth of transplanted neural progenitors derived from human-induced pluripotent stem cells. Stem Cells Dev 22: 374–382.

45. Bertrand N, DS Castro and F Guillemot. (2002). Proneural genes and the specification of neural cell types. Nat Rev Neurosci 3:517–530.
46. Barberi T, M Bradbury, Z Dincer, G Panagiotakos, ND Socci, et al. (2007). Derivation of engraftable skeletal myoblasts from human embryonic stem cells. Nat Med 13:642–648.
47. Perrier AL, V Tabar, T Barberi, ME Rubio, J Bruses, et al. (2004). Derivation of midbrain dopamine neurons from human embryonic stem cells. Proc Natl Acad Sci U S A 101:12543–12548.
48. Chung S, JI Moon, A Leung, D Aldrich, S Lukianov, et al. (2011). ES cell-derived renewable and functional midbrain dopaminergic progenitors. Proc Natl Acad Sci U S A 108: 9703–9708.

Address correspondence to:
Vannary Tieng
Department of Pathology and Immunology
University Medical Center
University of Geneva
rue Michel Servet 1
CH-1211 Geneva 4
Switzerland

E-mail: vannary.tiengcaulet@unige.ch

Received for publication September 17, 2013
Accepted after revision February 27, 2014
Prepublished on Liebert Instant Online February 27, 2014